

SNHG3 cooperates with ELAVL2 to modulate cell apoptosis and extracellular matrix accumulation by stabilizing SNAI2 in human trabecular meshwork cells under oxidative stress

Sizhen Li

Nanjing Tongren Hospital

Qingsong Yang (✉ doctor.yangqs@hotmail.com)

Nanjing Tongren Hospital <https://orcid.org/0000-0003-2904-1503>

Zixiu Zhou

Nanjing Tongren Hospital

Min Fu

Nanjing Tongren Hospital

Xiaodong Yang

Nanjing Tongren Hospital

Kuanxiao Hao

Nanjing Tongren Hospital

Yating Liu

Nanjing Tongren Hospital

Research article

Keywords: SNHG3, ELAVL2, SNAI2, trabecular meshwork cells, extracellular matrix accumulation

Posted Date: December 22nd, 2020

DOI: <https://doi.org/10.21203/rs.3.rs-130712/v1>

License:  This work is licensed under a Creative Commons Attribution 4.0 International License.

[Read Full License](#)

Abstract

Background: Glaucoma is the main reason for irreversible blindness, and pathological increased intraocular pressure is the leading risk factor for glaucoma. It is reported that trabecular meshwork cell injury is closely associated with the elevated intraocular pressure. The current study aimed to investigate the role of SNHG3 in human trabecular meshwork (HTM) cells under oxidative stress.

Methods: A series of experiments including real-time quantitative polymerase chain reaction (RT-qPCR), subcellular fractionation assay, western blot analysis, cell counting kit-8 (CCK-8) assay, RNA pull down, flow cytometry analysis, and RIP assay were employed to explore the biological function and regulatory mechanism of SNHG3 in HTM cells under oxidative stress.

Results: First, we observed that H₂O₂ induced SNHG3 upregulation in HTM cells. Then, we found that SNHG3 silencing alleviated H₂O₂-induced oxidative damage in HTM cells. Moreover, SNAI2 knockdown alleviated the oxidative damage induced by H₂O₂ in HTM cells. Mechanistically, SNHG3 bound with ELAVL2 to stabilize SNAI2. Finally, SNAI2 overexpression counteracted the effect of SNHG3 silencing on H₂O₂-induced HTM cells.

Conclusion: Our results demonstrated that SNHG3 cooperated with ELAVL2 to modulate cell apoptosis and extracellular matrix (ECM) accumulation by stabilizing SNAI2 in HTM cells under oxidative stress.

Introduction

Glaucoma is characterized by atrophy and depression of optic papilla, visual field defect and visual acuity decline^{1,2}. Pathological elevation of intraocular pressure and inadequate blood supply of optic nerve are the main reasons for glaucoma^{3,4}. Previous research has showed that trabecular meshwork (TM) cells exert crucial effect on aqueous humour circulation, and TM cell injury is closely related to the elevated intraocular pressure^{5,6}. Hence, finding novel biomarkers that modulate human trabecular meshwork (HTM) cell injury in glaucomatous patients is of vital significance.

In primary open angle glaucoma, increased intraocular pressure results in deformation at the optic nerve head; especially, intraocular pressure elevation leads to the deformation at the lamina cribrosa region where extracellular matrix (ECM) molecules such as fibronectin and collagen tend to accumulate⁷⁻⁹. Changes in the levels of regulators of ECM homeostasis such as matrix metalloproteinases (MMPs) occur in the primary open angle glaucoma lamina cribrosa¹⁰. MMPs are zinc-dependent endopeptidases, which degrade ECM components such as fibronectin and collagen^{11,12}. MMPs are crucial regulators of aqueous humor outflow for they can remodel TM ECM and keep a stable outflow resistance and ensuing intraocular pressure¹³⁻¹⁵. Therefore, MMPs are promising therapeutic targets for glaucoma treatment due to their capability to regulate aqueous humor outflow^{13,14}.

Long noncoding RNAs (lncRNAs) are a category of noncoding RNAs (ncRNAs), with over 200 nucleotides in size^{16,17}. LncRNAs are related to multiple cellular functions, and most of the cellular functions involve the binding of lncRNAs with one or more RNA-binding proteins (RBPs) to increase the stability of target messenger RNAs (mRNAs)¹⁸⁻²¹. LncRNAs are active regulators in a variety of diseases, including glaucoma²²⁻²⁴. For example, lncRNA GAS5 knockdown relieves glaucoma in rat models via decreasing the apoptosis of retinal ganglion cells²⁵. LncRNA MALAT1 regulates the apoptosis of retinal ganglion cells via the PI3K/Akt pathway in glaucomatous rats²⁶. LncRNA MEG3 participates in glaucoma progression by facilitating the autophagy of retinal ganglion cells²⁷. LncRNA SNHG3 (small nucleolar RNA host gene 3) has been found to participate in regulating the development of several diseases²⁸⁻³⁰. Importantly, SNHG3 has been found to be related to neurodegeneration³¹, and it has been reported to be upregulated in H₂O₂-induced HTM cells³². Accordingly, we predicted that SNHG3 may exert certain effect on glaucoma.

DNA damage is related to various neurodegenerative diseases, including glaucoma^{32,33}. In comparison with healthy controls, oxidative DNA damage is distinctly increased in the TM of patients with glaucoma³². In this study, a H₂O₂-induced oxidative damage HTM cell model was established and the role of SNHG3 in H₂O₂-induced HTM cells was explored. Our investigation may provide a novel direction for the treatment of glaucoma.

Materials And Methods

Cell lines and cell culture

HTM cells were acquired from cadaver eyes with the approval of the Ethics Committee of Nanjing Tongren Hospital (Jiangsu, China). HTM cells were incubated in Dulbecco's modified Eagle's medium (DMEM; USA) containing 10% fetal bovine serum (FBS; Invitrogen, USA), 100 U/ml penicillin (Sigma-Aldrich, USA) and 100 µg/ml streptomycin (Sigma-Aldrich, USA), and then stored in the humidified atmosphere with 5% CO₂ at 37°C.

Cell treatment

The cultured HTM cells were treated with disparate concentrations of H₂O₂ (0 – 300 µM) to establish an *in vitro* oxidative cell damage model. Non-disposed cells acted as a control.

Cell transfection

For overexpression of SNAI2, the SNAI2 sequence was synthesized and inserted into the pcDNA3.1 (Invitrogen, U.S.A.) plasmid to produce the pcDNA3.1/SNAI2. For knockdown of SNHG3, SNAI2 or ELAVL2, short hairpin RNA (shRNA) specifically targeting SNHG3, SNAI2 or ELAVL2 were devised and synthesized by GenePharma (Shanghai, China). Lipofectamine 2000 (Invitrogen, U.S.A.) was applied for cell transfection in line with manufacturer's recommendations.

CCK-8 assay

The viability of HTM cells were detected by using Cell Counting Kit-8 (CCK-8). The transfected cells with 1×10^4 cells per well were planted in 96-well plates. After incubation for 48 h, CCK-8 solution (10 μ l) was supplemented into each well. After that, the incubation continued for 4 h. Cell viability was visualized using a microplate reader (EL340; BioTek Instruments, Hopkinton, MA) at a wavelength of 450 nm.

Flow cytometry analysis

The flow cytometry was conducted to assess HTM cell apoptosis with Annexin V Kit (Beyotime, China) with reference to protocols stipulated by the manufacturer. Cells transfected with indicated plasmid or negative control were collected 48 h later and washed twice with PBS. Subsequently, cells (1×10^6 cells/mL) were double stained by propidium iodide (PI) and Annexin V-FITC. The CELLQUEST program (Becton Dickinson, USA) was used to record cells.

Western blot

Transfected cells were lysed applying RIPA buffer (Thermo, USA), and cultured for 15 min at 4°C. Then, the lysate was centrifuged, and the concentrations of the proteins were measured using an BCA Protein Assay Kit (Thermo, USA). The proteins were isolated on 10% sodium dodecyl sulfate polyacrylamide gel electrophoresis (SDS-PAGE) and moved onto PVDF membranes (Thermo, USA). Then, 5% skim milk was used to block the membranes for 1 h. Next, the membranes were incubated with primary antibodies overnight at 4°C. The primary antibodies were obtained from Abcam company (Shanghai, China): SNAI2 (ab51772), ELAVL2 (ab72603), collagen α 1 (ab34710), fibronectin (ab2413), collagen III (ab7778), MMP3 (ab52915), MMP9 (ab76003) and GAPDH (ab8245). Subsequently, secondary antibody was used to be incubated with the membranes for 2 h at room temperature. Finally, an enhanced chemiluminescence kit (GE Healthcare, Chicago, IL) was adopted to observe the signals.

Real-time quantitative polymerase chain reaction (RT-qPCR)

TRIzol reagent (ThermoFisher Scientific Invitrogen, USA) was employed to extract total RNA. Then, total RNA was reverse transcribed to cDNA using the High Capacity cDNA Reverse Transcription Kits (Applied Biosystems, Foster City, CA, USA). RT-qPCR analysis was performed using a SYBR Premix Ex Taq II kit (Cat. #RR820A, TaKaRa) on the 7500 Real-Time PCR Systems (Applied Biosystems). U6 served as an endogenous control for miRNAs. The detection results for mRNAs were normalized to GAPDH. Expression fold changes were calculated adopting the $2^{-\Delta\Delta C_t}$ method.

Subcellular fractionation assay

Total RNA was extracted applying a DNA/RNA Isolation Kit (DP422, Tiangen Biotech, Beijing, China) in line with the instruction. The nuclear and cytoplasmic fractions were separated applying NE-PER Nuclear and Cytoplasmic Extraction Reagents (Thermo Scientific). Total RNA was isolated from the nuclear and cytoplasmic fractions using Trizol (Invitrogen).

RNA pull down assay

The biotinylated RNAs were cultured with cell lysates, and then cultured with streptavidin beads (Invitrogen). Subsequently, the RNAs in complexes captured by streptavidin beads were washed, purified and assessed by western blot analysis.

RNA immunoprecipitation (RIP) assay

The RIP assay was carried out with a Millipore EZ-Magna RIP RNA-Binding Protein Immunoprecipitation kit (Millipore, Bedford, MA, USA). The precipitated RNAs were evaluated using RT-qPCR. Antibodies against ELAVL2 and IgG were used. IgG served as the negative control.

Data statistics

Data analysis was conducted using SPSS 23.0 (IBM SPSS, Chicago, IL, USA). All data are exhibited as the means \pm SD. Statistical significance among more than 2 groups was calculated using one-way ANOVA and Tukey's post-hoc test. Difference between 2 groups was evaluated using Student's t-test. $P < 0.05$ was regarded to be statistically significant.

Results

H₂O₂ induced SNHG3 upregulation in HTM cells

We first established a H₂O₂-induced oxidative damage model in HTM cells. Then, HTM cells were treated with different concentrations of H₂O₂ (0, 100, 200, and 300 μ M). Next, the viability and apoptosis of H₂O₂-induced HTM cells were detected. CCK-8 assay revealed that HTM cell viability was inhibited by H₂O₂ at the concentrations of 100 μ M, 200 μ M and 300 μ M (Fig. 1A). Since the IC₅₀ of viability was exhibited at the concentration of 200 μ M, we chose 200 μ M H₂O₂ to dispose HTM cells in the subsequent assays. Flow cytometry analysis showed H₂O₂ induced the apoptosis of HTM cells compared with the control group (Fig. 1B). Additionally, the levels of extracellular matrix (ECM) proteins Collagen I, Collagen III, Fibronectin, MMP3, and MMP9 were obviously increased by H₂O₂ in HTM cells (Fig. 1C). Moreover, SNHG3 expression was upregulated in HTM cells (Fig. 1D). In summary, these data showed that the H₂O₂-induced oxidative damage model in HTM cells was established successfully.

SNHG3 silencing alleviated H₂O₂-induced oxidative damage in HTM cells

To detect the biological function of SNHG3 in H₂O₂-induced HTM cells, SNHG3 was knockdown by transfection of sh-SNHG3#1 or sh-SNHG3#2 (Fig. 2A). Then, CCK-8 assay demonstrated SNHG3 knockdown promoted the viability of H₂O₂-induced HTM cells (Fig. 2B). Flow cytometry analysis showed that SNHG3 silencing suppressed the apoptosis of H₂O₂-induced HTM cells (Fig. 2C). Moreover, the levels of ECM proteins Collagen III, Collagen I, Fibronectin, MMP3, and MMP9 were reduced by SNHG3 silencing

in H₂O₂-induced HTM cells (Fig. 2D). Overall, SNHG3 silencing alleviated H₂O₂-induced oxidative damage in HTM cells.

SNAI2 knockdown alleviated H₂O₂-induced oxidative damage in HTM cells

SNAI2 has been widely reported to regulate ECM proteins^{34,35}, so we predicted that it regulated ECM proteins in HTM cells. To evaluate the biological function of SNAI2 in H₂O₂-induced HTM cells, SNAI2 was knockdown by transfection of sh-SNAI2#1 or sh-SNAI2#2. Western blot analysis demonstrated that SNAI2 protein level was increased by H₂O₂, but it was then decreased by transfection of sh-SNAI2#1 or sh-SNAI2#2 (Fig. 3A). Then, CCK-8 assay showed SNAI2 knockdown promoted the viability of H₂O₂-induced HTM cells (Fig. 4B). Flow cytometry analysis revealed that SNAI2 knockdown suppressed the apoptosis of H₂O₂-induced HTM cells (Fig. 3C). Moreover, the levels of ECM proteins Collagen III, Collagen I, Fibronectin, MMP3, and MMP9 were reduced by SNAI2 knockdown in H₂O₂-induced HTM cells (Fig. 3D). In summary, SNAI2 silencing alleviated H₂O₂-induced oxidative damage in HTM cells.

SNHG3 bound with ELAVL2 to stabilize SNAI2

Subsequently, we explored the molecular mechanism of SNHG3 in HTM cells. First, we found that SNHG3 mainly existed in the cytoplasm of cells by using online tool (<http://www.csbio.sjtu.edu.cn/bioinf/IncLocator/>) (Fig. 4A). Then, we further found that SNHG3 mainly existed in the cytoplasm of HTM cells (Fig. 4B). Next, as shown in Fig. 4C, by searching the website <http://rbpdb.ccr.utoronto.ca>, one RBP, ELAVL2, was identified to bind with SNHG3 and SNAI2 (condition: binding score > 10). Based on the website <http://pridb.gdcb.iastate.edu//RPISeq/>, the accuracies of random forest (RF) and support vector machine (SVM) classifiers for SNHG3-ELAVL2 binding were 0.9 and 0.91 respectively, and the accuracies of RF and SVM classifiers for SNAI2 3'UTR-ELAVL2 binding were 0.65 and 0.96 respectively, suggesting ELAVL2 bound with SNHG3 and SNAI2 (Fig. 4D). RNA pull down assay demonstrated that ELAVL2 was enriched in the Bio-SNHG3 sense group and the Bio-SNAI2 sense group but not the Bio-SNHG3 antisense group and Bio-SNAI2 antisense group, confirming that ELAVL2 bound with SNHG3 and SNAI2 (Fig. 4E). Similarly, RIP assay suggested that both SNHG3 and SNAI2 were enriched in the anti-ELAVL2 group instead of the anti-IgG group (Fig. 4F). Subsequently, HTM cells were transfected with sh-ELAVL2, showing the decreased ELAVL2 expression (Fig. 4G). Then, western blot analysis revealed that ELAVL2 or SNHG3 silencing reduced the protein level of SNAI2 in HTM cells (Fig. 4H-I). Moreover, ELAVL2 silencing or SNHG3 silencing decreased SNAI2 mRNA half-life (Fig. 4J). Overall, SNHG3 bound with ELAVL2 to stabilize SNAI2.

SNAI2 overexpression counteracted the effect of SNHG3 silencing on H₂O₂-induced HTM cells

To detect whether SNAI2 overexpression counteracted the effect of SNHG3 silencing on HTM cells, rescue assays were conducted. First, SNAI2 protein level was elevated by the transfection of pcDNA3.1/SNAI2 in H₂O₂-induced HTM cells (Fig. 5A). Then, we found that SNAI2 overexpression counteracted the promotive effect of SNHG3 silencing on H₂O₂-induced HTM cell viability (Fig. 5B). SNAI2 overexpression offset the

inhibitive effect of SNHG3 silencing on H₂O₂-induced HTM cell apoptosis (Fig. 5C). Additionally, the suppressive influence of SNHG3 knockdown on ECM proteins (Collagen I, Collagen III, Fibronectin, MMP3, and MMP9) was abolished by SNAI2 overexpression (Fig. 5D). In conclusion, SNAI2 overexpression abrogated the effect of SNHG3 silencing on H₂O₂-induced HTM cells.

Discussion

In this research, we established a H₂O₂-induced oxidative damage model in HTM cells and explored the role of SNHG3 in H₂O₂-induced HTM cells. Our data suggested that SNHG3 cooperated with ELAVL2 to modulate cell apoptosis and ECM accumulation by stabilizing SNAI2 in H₂O₂-induced HTM cells.

Previous research demonstrated that lncRNAs have been implicated in neurodegenerative diseases, including Alzheimer's disease^{36,37} and glaucoma^{23,24}. SNHG3 has been reported to regulate a variety of diseases, such as hepatocellular carcinoma²⁹ and osteosarcoma³⁰. Notably, SNHG3 has been found to be related to neurodegeneration³¹, and it has been reported to be upregulated in H₂O₂-induced HTM cells³². In the present study, our data revealed that SNHG3 was upregulated in H₂O₂-induced HTM cells and SNHG3 silencing alleviated H₂O₂-induced oxidative damage in HTM cells by promoting cell viability, inhibiting cell apoptosis and decreasing ECM protein level.

SNAI2 (snail family transcriptional repressor 2) is also known as SLUG, SLUGH, SLUGH1, SNAIL2, or WS2D; it has been reported to regulate a wide range of human diseases³⁸⁻⁴⁰. Importantly, previous research has proved that SNAI2 is involved in the regulation of neurodegenerative diseases⁴¹, and it may participate in the modulation of glaucoma⁴². However, the specific role and regulatory mechanism of SNAI2 in glaucoma is not clear.

lncRNAs can cooperate with specific proteins to increase mRNA stability or induce mRNA decay in cytoplasm⁴³. For example, lncRNA LINC00707 interacts with mRNA stabilizing protein HuR to increase the stability of VAV3/F11R in gastric cancer⁴⁴. lncRNA LAST interacts with CNBP to promote CCND1 mRNA stability in human cells⁴⁵. Previously, the regulatory mechanism of SNHG3 has been explored in some human diseases^{29,30,46}. However, the molecular regulatory mechanism of SNHG3 in glaucoma remains to be explored. In this study, we observed that SNHG3 bound with ELAVL2 to stabilize SNAI2 in H₂O₂-induced HTM cells. SNAI2 overexpression counteracted the effect of SNHG3 silencing on H₂O₂-induced HTM cells. In addition, we found that SNAI2 knockdown relieved H₂O₂-induced oxidative damage in HTM cells by promoting cell viability, inhibiting cell apoptosis and decreasing ECM protein level.

Conclusions

The main purpose of the present research was to investigate the biological role and regulatory mechanism of SNHG3 in H₂O₂-induced HTM cells. Our results illustrated that SNHG3 interacted with ELAVL2 to regulate cell proliferation, apoptosis and ECM accumulation by increasing the stability of

SNAI2 in H₂O₂-induced HTM cells. This finding may shed some light on the regulatory mechanism of SNHG3 in human diseases and advance our understanding on the pathogenesis of glaucoma. Future studies should be conducted on the biological functions of SNHG3 in other cell types and the regulatory mechanism of H₂O₂-induced dysregulated SNHG3 expression. In addition, *in vivo* experiments could be added to further validate the role of SNHG3 in glaucoma.

Abbreviations

HTM: human trabecular meshwork; RT-qPCR: real-time quantitative polymerase chain reaction; CCK-8: cell counting kit-8; ECM: extracellular matrix; TM: trabecular meshwork; MMPs: matrix metalloproteinases; lncRNAs: long noncoding RNAs; ncRNAs: noncoding RNAs; RBPs: RNA-binding proteins; mRNAs: messenger RNAs; RIP: RNA immunoprecipitation;

Declarations

Ethical Approval and Consent to participate

Not applicable

Consent for publication

Not applicable

Availability of supporting data

The data underlying this article will be shared on reasonable request to the corresponding author.

Acknowledgement

Not applicable.

Funding

None

Conflicts of interest

The authors declare that there are no competing interests in this study.

Authors' contributions

Sizhen Li conceived and designed the experiments. Sizhen Li, Qingsong Yang, Zixiu Zhou, Min Fu, Xiaodong Yang, Kuanxiao Hao, and Yating Liu carried out the experiments. Sizhen Li and Qingsong Yang analyzed the data. Sizhen Li and Qingsong Yang drafted the manuscript. All authors agreed to be accountable for all aspects of the work. All authors have read and approved the final manuscript.

References

1. He S, Stankowska DL, Ellis DZ, Krishnamoorthy RR, Yorio T. Targets of Neuroprotection in Glaucoma. *Journal of ocular pharmacology and therapeutics : the official journal of the Association for Ocular Pharmacology and Therapeutics*. 2018;34(1-2):85-106.
2. Weinreb RN, Aung T, Medeiros FA. The pathophysiology and treatment of glaucoma: a review. *Jama*. 2014;311(18):1901-1911.
3. Jonas JB, Aung T, Bourne RR, Bron AM, Ritch R, Panda-Jonas S. Glaucoma. *Lancet (London, England)*. 2017;390(10108):2183-2193.
4. Patel N, McAllister F, Pardon L, Harwerth R. The effects of graded intraocular pressure challenge on the optic nerve head. *Experimental eye research*. 2018;169:79-90.
5. Agarwal P, Agarwal R. Trabecular meshwork ECM remodeling in glaucoma: could RAS be a target? *Expert opinion on therapeutic targets*. 2018;22(7):629-638.
6. Saccà SC, Gandolfi S, Bagnis A, et al. From DNA damage to functional changes of the trabecular meshwork in aging and glaucoma. *Ageing research reviews*. 2016;29:26-41.
7. Nikhalashree S, George R, Shantha B, et al. Detection of Proteins Associated with Extracellular Matrix Regulation in the Aqueous Humour of Patients with Primary Glaucoma. *Current eye research*. 2019;44(9):1018-1025.
8. NikhalaShree S, Karthikkeyan G, George R, et al. Lowered Decorin With Aberrant Extracellular Matrix Remodeling in Aqueous Humor and Tenon's Tissue From Primary Glaucoma Patients. *Investigative ophthalmology & visual science*. 2019;60(14):4661-4669.
9. Tamm ER, Fuchshofer R. What increases outflow resistance in primary open-angle glaucoma? *Survey of ophthalmology*. 2007;52 Suppl 2:S101-104.
10. Rönkkö S, Rekonen P, Kaarniranta K, Puustjärvi T, Teräsvirta M, Uusitalo H. Matrix metalloproteinases and their inhibitors in the chamber angle of normal eyes and patients with primary open-angle glaucoma and exfoliation glaucoma. *Graefes archive for clinical and experimental ophthalmology = Albrecht von Graefes Archiv fur klinische und experimentelle Ophthalmologie*. 2007;245(5):697-704.
11. Hrabec E, Naduk J, Strek M, Hrabec Z. [Type IV collagenases (MMP-2 and MMP-9) and their substrates—intracellular proteins, hormones, cytokines, chemokines and their receptors]. *Postepy biochemii*. 2007;53(1):37-45.
12. Polette M, Birembaut P. Membrane-type metalloproteinases in tumor invasion. *The international journal of biochemistry & cell biology*. 1998;30(11):1195-1202.
13. Wallace DM, Murphy-Ullrich JE, Downs JC, O'Brien CJ. The role of matricellular proteins in glaucoma. *Matrix biology : journal of the International Society for Matrix Biology*. 2014;37:174-182.
14. Wallace DM, Pokrovskaya O, O'Brien CJ. The Function of Matricellular Proteins in the Lamina Cribrosa and Trabecular Meshwork in Glaucoma. *Journal of ocular pharmacology and therapeutics : the official journal of the Association for Ocular Pharmacology and Therapeutics*. 2015;31(7):386-395.

15. Chatterjee A, Villarreal G, Jr, Rhee DJ. Matricellular proteins in the trabecular meshwork: review and update. *Journal of ocular pharmacology and therapeutics : the official journal of the Association for Ocular Pharmacology and Therapeutics*. 2014;30(6):447-463.
16. DiStefano JK. The Emerging Role of Long Noncoding RNAs in Human Disease. *Methods in molecular biology (Clifton, NJ)*. 2018;1706:91-110.
17. Lee H, Zhang Z, Krause HM. Long Noncoding RNAs and Repetitive Elements: Junk or Intimate Evolutionary Partners? *Trends in genetics : TIG*. 2019;35(12):892-902.
18. Ferrè F, Colantoni A, Helmer-Citterich M. Revealing protein-lncRNA interaction. *Briefings in bioinformatics*. 2016;17(1):106-116.
19. Fasolo F, Patrucco L, Volpe M, et al. The RNA-binding protein ILF3 binds to transposable element sequences in SINEUP lncRNAs. *FASEB journal : official publication of the Federation of American Societies for Experimental Biology*. 2019;33(12):13572-13589.
20. Lee S, Kopp F, Chang TC, et al. Noncoding RNA NORAD Regulates Genomic Stability by Sequestering PUMILIO Proteins. *Cell*. 2016;164(1-2):69-80.
21. Ramanathan M, Porter DF, Khavari PA. Methods to study RNA-protein interactions. *Nature methods*. 2019;16(3):225-234.
22. Cissé Y, Bai L, Chen MT. LncRNAs in ocular neovascularizations. *International journal of ophthalmology*. 2019;12(12):1959-1965.
23. Cissé Y, Bai L, Meng T. LncRNAs in genetic basis of glaucoma. *BMJ open ophthalmology*. 2018;3(1):e000131.
24. Wan P, Su W, Zhuo Y. The Role of Long Noncoding RNAs in Neurodegenerative Diseases. *Molecular neurobiology*. 2017;54(3):2012-2021.
25. Zhou RR, Li HB, You QS, et al. Silencing of GAS5 Alleviates Glaucoma in Rat Models by Reducing Retinal Ganglion Cell Apoptosis. *Human gene therapy*. 2019;30(12):1505-1519.
26. Li HB, You QS, Xu LX, et al. Long Non-Coding RNA-MALAT1 Mediates Retinal Ganglion Cell Apoptosis Through the PI3K/Akt Signaling Pathway in Rats with Glaucoma. *Cellular physiology and biochemistry : international journal of experimental cellular physiology, biochemistry, and pharmacology*. 2017;43(5):2117-2132.
27. Sun W, Li YN, Ye JF, Guan YQ, Li SJ. MEG3 is involved in the development of glaucoma through promoting the autophagy of retinal ganglion cells. *European review for medical and pharmacological sciences*. 2018;22(9):2534-2540.
28. Liu Z, Tao H. Small nucleolar RNA host gene 3 facilitates cell proliferation and migration in oral squamous cell carcinoma via targeting nuclear transcription factor Y subunit gamma. *Journal of cellular biochemistry*. 2020;121(3):2150-2158.
29. Zhang PF, Wang F, Wu J, et al. LncRNA SNHG3 induces EMT and sorafenib resistance by modulating the miR-128/CD151 pathway in hepatocellular carcinoma. *Journal of cellular physiology*. 2019;234(3):2788-2794.

30. Zheng S, Jiang F, Ge D, et al. LncRNA SNHG3/miRNA-151a-3p/RAB22A axis regulates invasion and migration of osteosarcoma. *Biomedicine & pharmacotherapy = Biomedecine & pharmacotherapie*. 2019;112:108695.
31. Arisi I, D'Onofrio M, Brandi R, et al. Gene expression biomarkers in the brain of a mouse model for Alzheimer's disease: mining of microarray data by logic classification and feature selection. *Journal of Alzheimer's disease : JAD*. 2011;24(4):721-738.
32. Yao K, Yu Y, Li F, Jin P, Deng C, Zhang H. Integrative analysis of an lncRNA-associated competing endogenous RNA network in human trabecular meshwork cells under oxidative stress. *Molecular medicine reports*. 2020;21(3):1606-1614.
33. Sáez GT. DNA Damage and Repair in Degenerative Diseases 2016. *International journal of molecular sciences*. 2017;18(1).
34. Cheon DJ, Tong Y, Sim MS, et al. A collagen-remodeling gene signature regulated by TGF- β signaling is associated with metastasis and poor survival in serous ovarian cancer. *Clinical cancer research : an official journal of the American Association for Cancer Research*. 2014;20(3):711-723.
35. Liu T, Zhang H, Sun L, et al. FSIP1 binds HER2 directly to regulate breast cancer growth and invasiveness. *Proceedings of the National Academy of Sciences of the United States of America*. 2017;114(29):7683-7688.
36. Luo Q, Chen Y. Long noncoding RNAs and Alzheimer's disease. *Clinical interventions in aging*. 2016;11:867-872.
37. Riva P, Ratti A, Venturin M. The Long Non-Coding RNAs in Neurodegenerative Diseases: Novel Mechanisms of Pathogenesis. *Current Alzheimer research*. 2016;13(11):1219-1231.
38. Pingault V, Ente D, Dastot-Le Moal F, Goossens M, Marlin S, Bondurand N. Review and update of mutations causing Waardenburg syndrome. *Human mutation*. 2010;31(4):391-406.
39. Nakayama Y, Tsuruya Y, Noda K, et al. Negative feedback by SNAI2 regulates TGF β 1-induced amelotin gene transcription in epithelial-mesenchymal transition. *Journal of cellular physiology*. 2019;234(7):11474-11489.
40. Zhou W, Gross KM, Kuperwasser C. Molecular regulation of Snai2 in development and disease. *Journal of cell science*. 2019;132(23).
41. Santana MM, Chung KF, Vukicevic V, et al. Isolation, characterization, and differentiation of progenitor cells from human adult adrenal medulla. *Stem cells translational medicine*. 2012;1(11):783-791.
42. Pattabiraman PP, Maddala R, Rao PV. Regulation of plasticity and fibrogenic activity of trabecular meshwork cells by Rho GTPase signaling. *Journal of cellular physiology*. 2014;229(7):927-942.
43. Gong C, Maquat LE. lncRNAs transactivate STAU1-mediated mRNA decay by duplexing with 3' UTRs via Alu elements. *Nature*. 2011;470(7333):284-288.
44. Xie M, Ma T, Xue J, et al. The long intergenic non-protein coding RNA 707 promotes proliferation and metastasis of gastric cancer by interacting with mRNA stabilizing protein HuR. *Cancer letters*. 2019;443:67-79.

45. Cao L, Zhang P, Li J, Wu M. LAST, a c-Myc-inducible long noncoding RNA, cooperates with CNBP to promote CCND1 mRNA stability in human cells. *eLife*. 2017;6.
46. Wang L, Su K, Wu H, Li J, Song D. LncRNA SNHG3 regulates laryngeal carcinoma proliferation and migration by modulating the miR-384/WEE1 axis. *Life sciences*. 2019;232:116597.

Figures

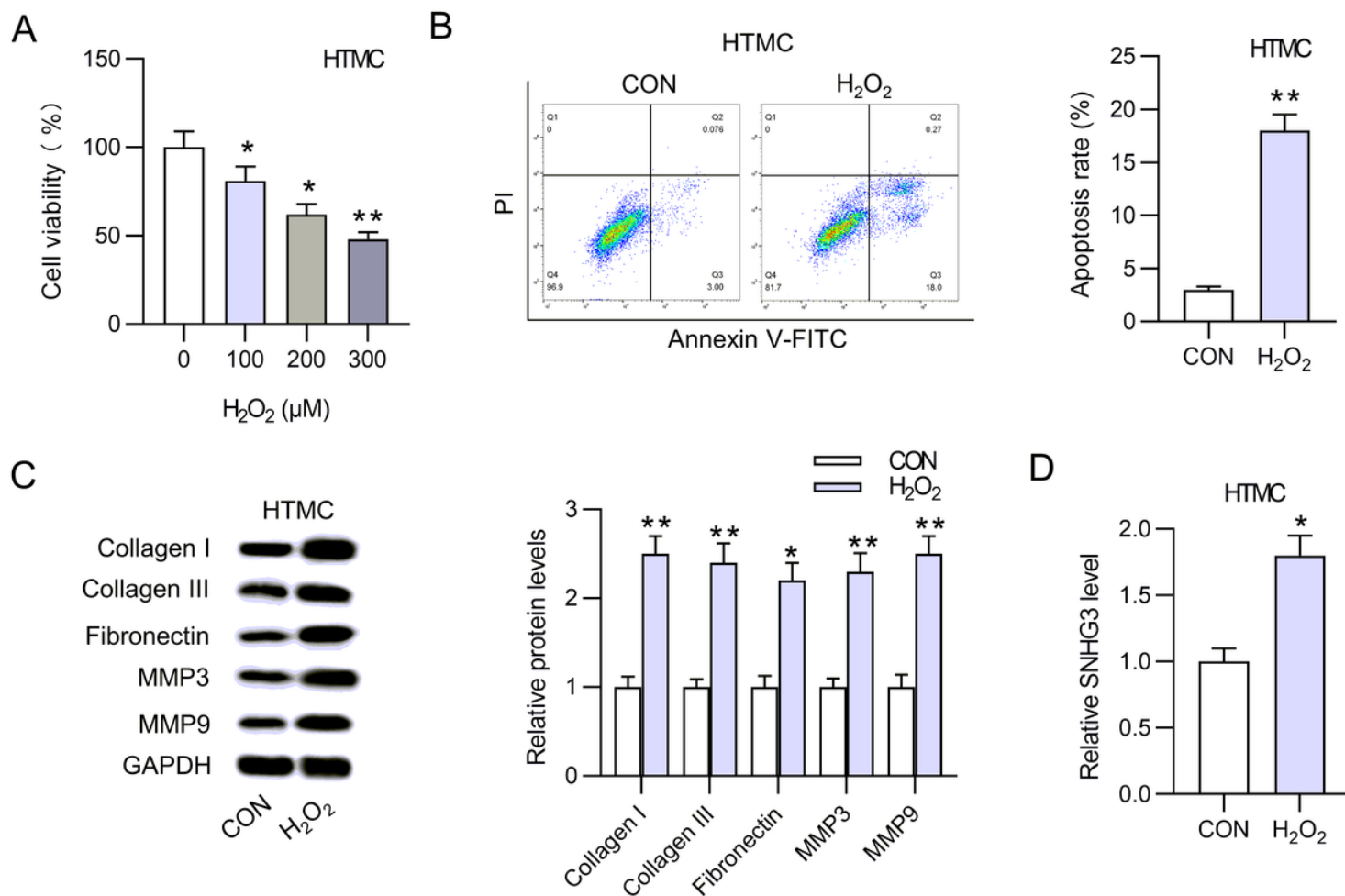


Figure 1

H₂O₂ induced SNHG3 upregulation in HTM cells. (A) HTM cell viability upon H₂O₂ at the concentrations of 100 μM, 200 μM and 300 μM was assessed by CCK-8 assay. (B) Flow cytometry analysis was used to detect the apoptosis of H₂O₂-induced HTM cells. (C) The levels of extracellular matrix (ECM) proteins Collagen I, Collagen III, Fibronectin, MMP3, and MMP9 were measured by western blot analysis. (D) The expression of SNHG3 was detected in H₂O₂-induced HTM cells *P< 0.05, **P< 0.01, ***P< 0.001.

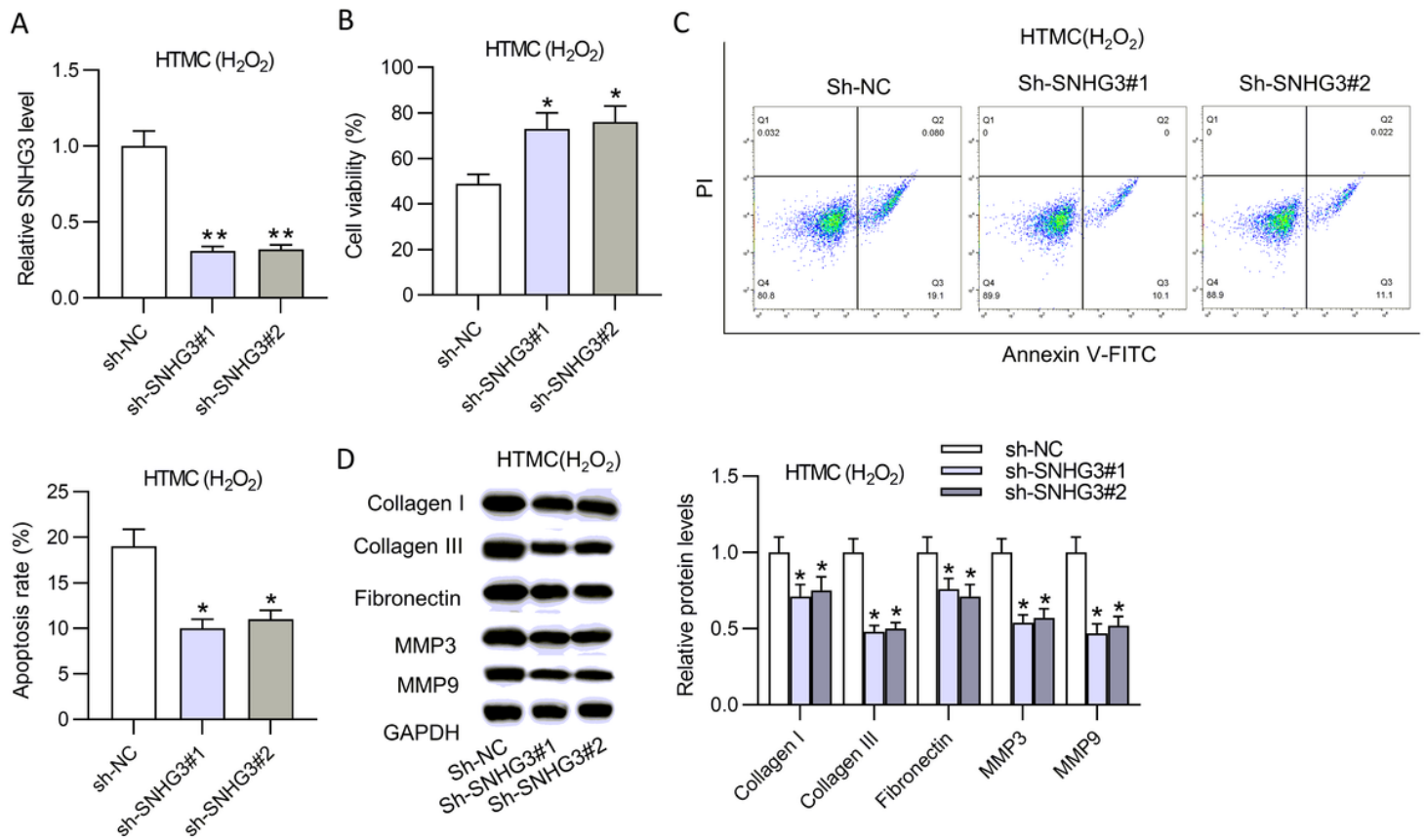


Figure 2

SNHG3 silencing alleviated H₂O₂-induced oxidative damage in HTM cells. (A) The knockdown efficiency of SNHG3 was assessed. (B) CCK-8 assay was used to evaluate the effect of SNHG3 silencing on the viability of H₂O₂-induced HTM cells. (C) Flow cytometry was performed to detect the apoptosis of H₂O₂-induced HTM cells after transfection of sh-SNHG3#1 or sh-SNHG3#2. (D) The Collagen I, Collagen III, Fibronectin, MMP3, and MMP9 proteins in H₂O₂-induced HTM cells after transfection of sh-SNHG3#1 or sh-SNHG3#2 were detected using western blot analysis. *P < 0.05, **P < 0.01, ***P < 0.001.

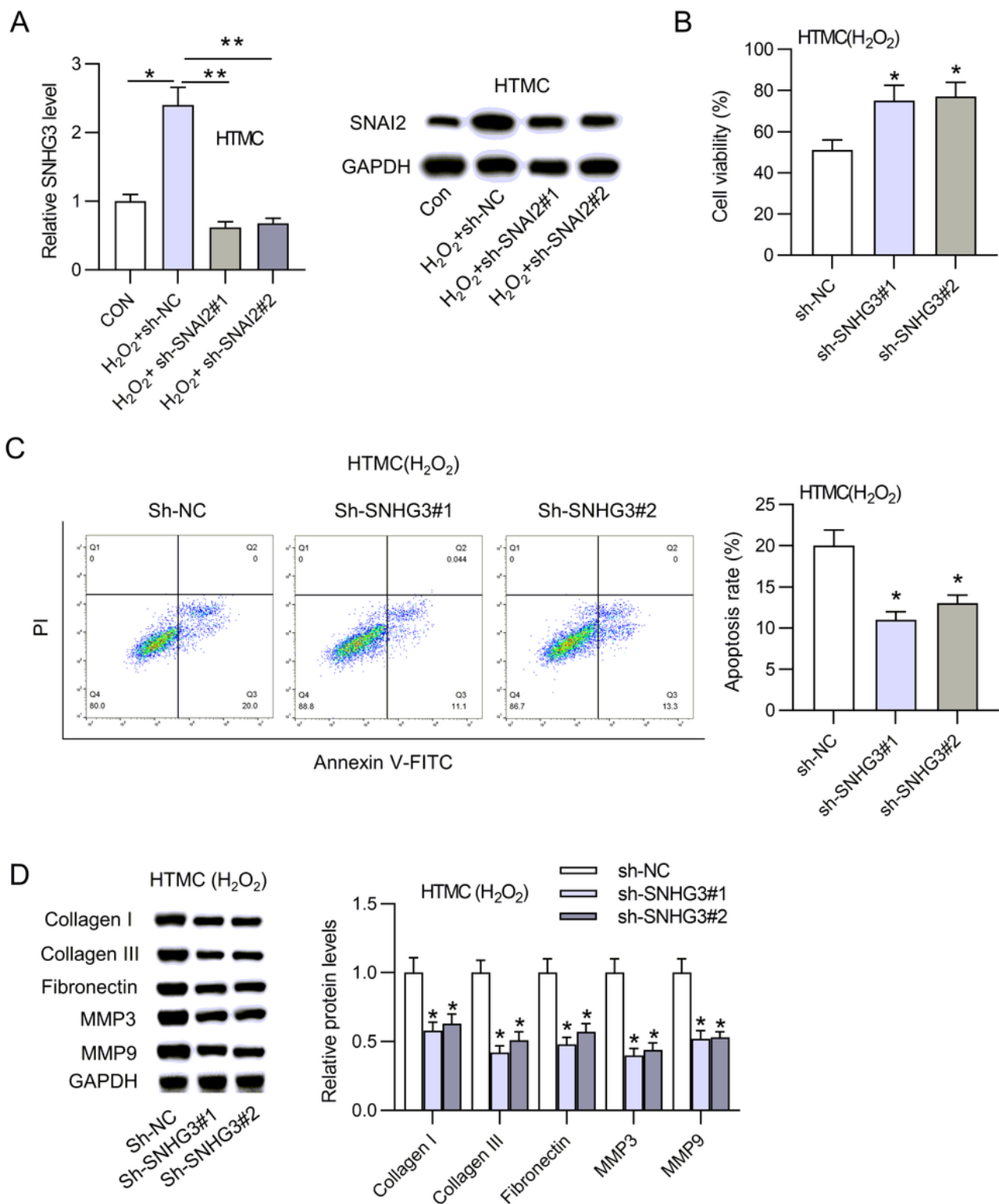


Figure 3

SNAI2 knockdown alleviated H₂O₂-induced oxidative damage in HTM cells. (A) The knockdown efficiency of SNAI2 was assessed. (B) CCK-8 assay was used to evaluate the effect of SNAI2 silencing on the viability of H₂O₂-induced HTM cells. (C) Flow cytometry was carried out to detect the apoptosis of H₂O₂-induced HTM cells upon sh-SNAI2#1 or sh-SNAI2#2. (D) The levels of ECM proteins (Collagen I,

Collagen III, Fibronectin, MMP3, and MMP9) in H2O2-induced HTM cells in response of sh-SNAI2#1 or sh-SNAI2#2. *P< 0.05, **P< 0.01, ***P< 0.001.

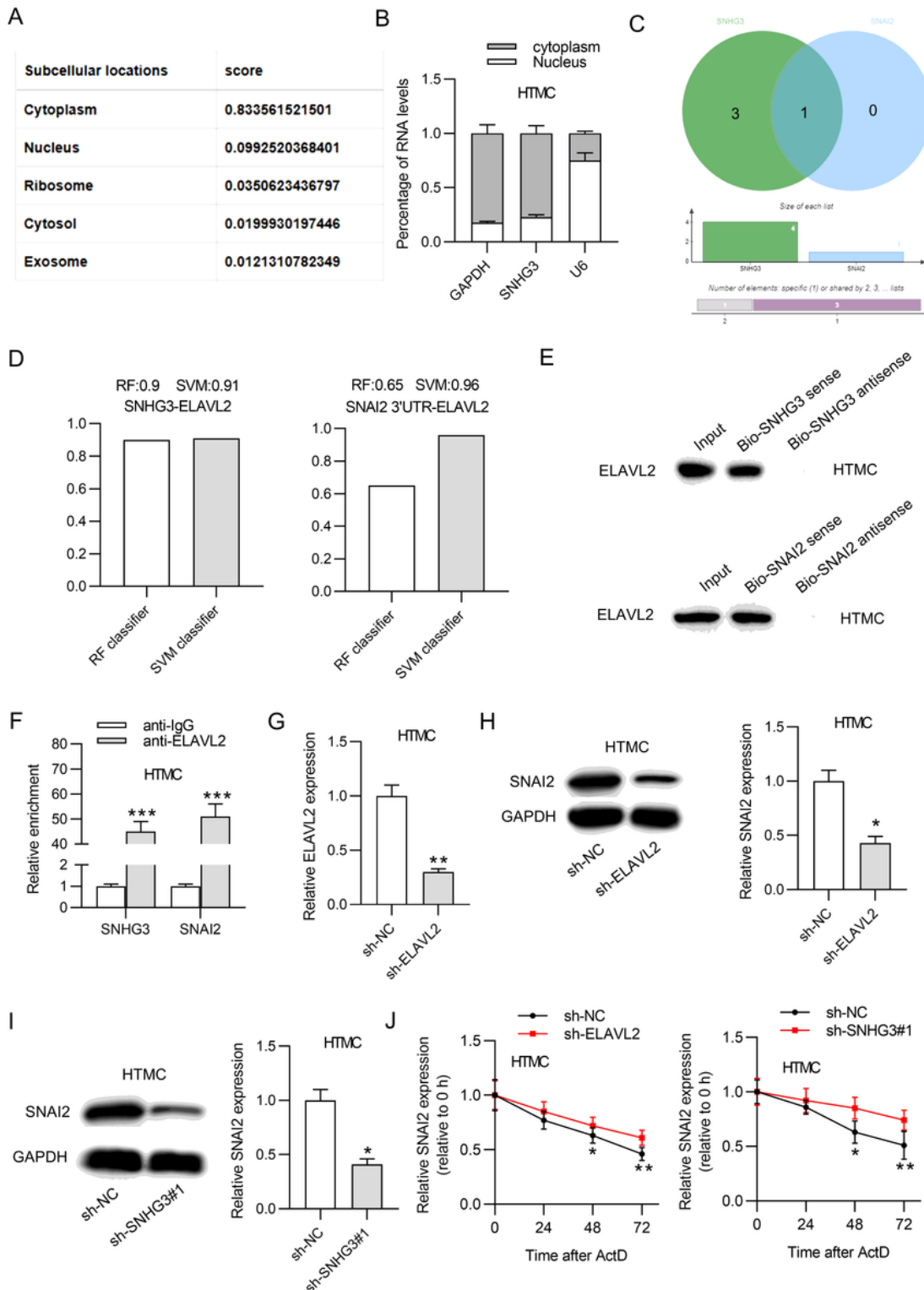


Figure 4

SNHG3 bound with ELAVL2 to stabilize SNAI2. (A) The location of SNHG3 in cells was identified by using the online tool (<http://www.csbio.sjtu.edu.cn/bioinf/IncLocator/>). (B) Subcellular fractionation assay was performed to localize SNHG3 in HTM cells. (C) Venn diagram exhibited the RBPs binding with SNHG3

and SNAI2. (D) Online database (<http://pridb.gdcb.iastate.edu//RPISeq/>) was used to analyze the binding ability of ELAVL2 with SNHG3 or SNAI2. (E) RNA pull down assay was conducted to assess the binding of ELAVL2 with SNHG3 or SNAI2. (F) RIP assay was used to evaluate the binding of ELAVL2 with SNHG3 or SNAI2. (G) The knockdown efficiency of ELAVL2 was detected. (H) The protein level of ELAVL2 in HTM cells after transfection of sh-ELAVL2. (I) The protein level of ELAVL2 in HTM cells after transfection of sh-SNHG3#1. (J) The expression of ELAVL2 in HTM cells after transfection of sh-ELAVL2 or sh-SNHG3#1. *P< 0.05, **P< 0.01, ***P< 0.001.

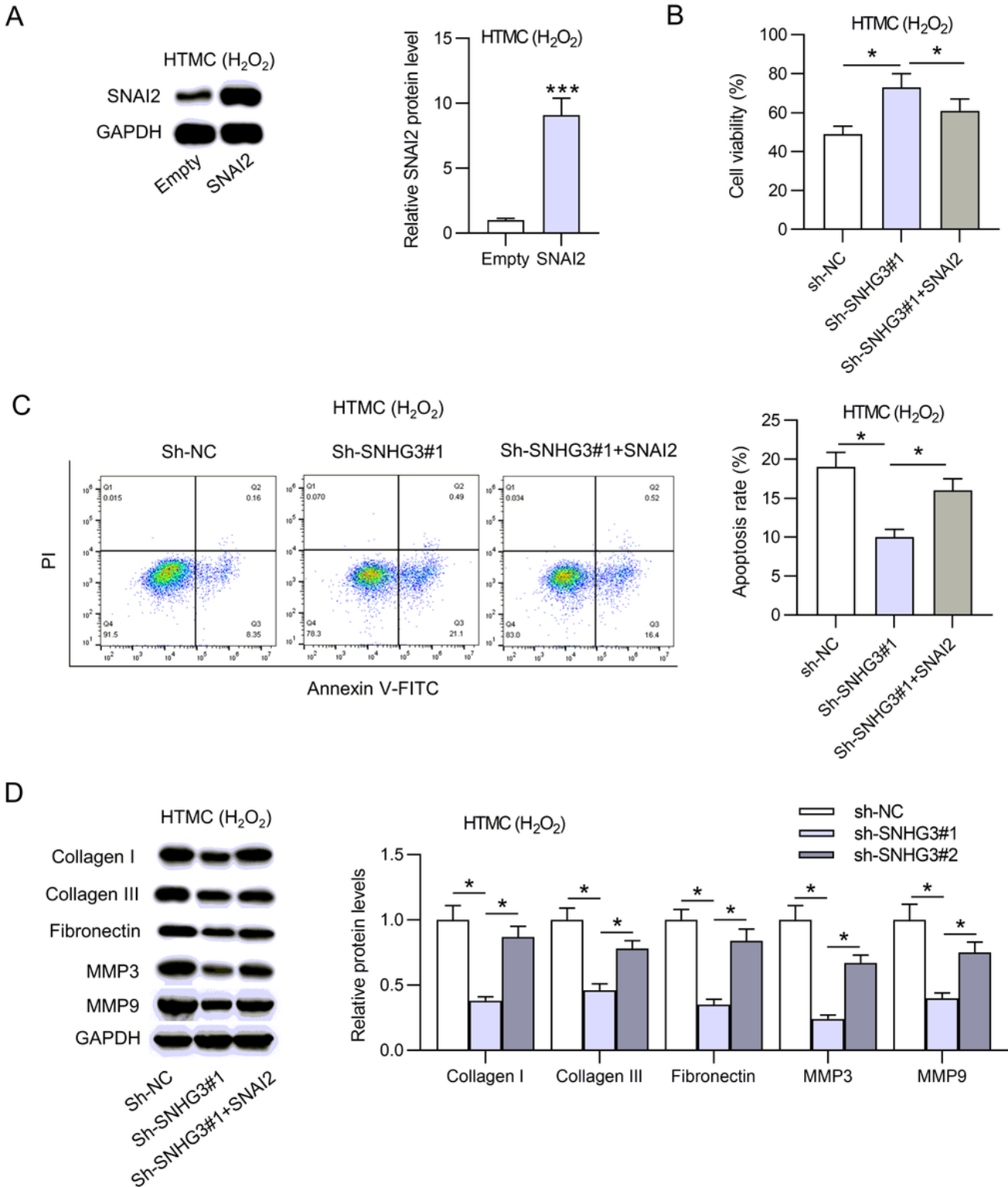


Figure 5

SNAI2 overexpression counteracted the effect of SNHG3 silencing on H₂O₂-induced HTM cells. (A) The overexpression efficiency of SNAI2 was assessed by western blot analysis. (B) The viability of H₂O₂-induced HTM cells after transfection of indicated plasmids was detected. (C) The apoptosis of H₂O₂-induced HTM cells after transfection of appointed plasmids. (D) The levels of ECM proteins (Collagen I, Collagen III, Fibronectin, MMP3, and MMP9) in H₂O₂-induced HTM cells in the different groups. *P < 0.05, **P < 0.01, ***P < 0.001.